View metadata, citation and similar papers at core.ac.uk

brought to you by CORE

provided by IntechOpen

We are IntechOpen, the world's leading publisher of Open Access books Built by scientists, for scientists

4,800
Open access books available

122,000
International authors and editors

135M
Downloads

Our authors are among the

154
Countries delivered to

TOP 1%
most cited scientists

12.2%
Contributors from top 500 universities

CLARIVATE ANALYTICS BOOK CITATION INDEX INDEXED

WEB OF SCIENCE™

Selection of our books indexed in the Book Citation Index in Web of Science™ Core Collection (BKCI)

Interested in publishing with us?
Contact book.department@intechopen.com

Numbers displayed above are based on latest data collected.
For more information visit www.intechopen.com

17

Human Ear Cartilage

Lu Zhang, Qiong Li, Yu Liu, Guangdong Zhou, Wei Liu and Yilin Cao
Department of Plastic and Reconstructive Surgery, Shanghai 9th People's Hospital, Shanghai Jiao Tong University School of Medicine, Shanghai Key Laboratory of Tissue Engineering, Shanghai P.R. China

1. Introduction

The human ear (Fig. 1) is of an ovoid form, with its larger end directed upward. Its lateral surface is irregularly concave, directed slightly forward, and presents numerous eminences and depressions to which names have been assigned (Beahm, Walton, 2002; Walton, Beahm, 2002). The prominent rim of the human ear is called the helix while another curved prominence, parallel with and in front of the helix, is called the antihelix; this divides above into two crura, between which is a triangular depression, the fossa triangularis. The narrow-curved depression between the helix and the antihelix is called the scapha; the antihelix describes a curve around a deep, capacious cavity, the concha, which is partially divided into two parts by the crus or commencement of the helix; the upper part is termed the cymba concha, the lower part the cavum concha. In front of the concha, and projecting backward over the meatus, is a small pointed eminence, the tragus, so called from its being generally covered on its under surface with a tuft of hair, resembling a goat's beard. Opposite the tragus, and separated from it by the intertragic notch, is a small tubercle, the antitragus. Below this is the lobule, composed of tough areolar and adipose tissues, and wanting the firmness and elasticity of the rest of the auricula.

Up to now, total human ear reconstruction for congenital microtia or auricular traumatic amputation still remains one of the greatest challenges for plastic surgeons(Brent, 1999; Nagata, 1993; TANZER, 1959). Although tissue engineering is a promising method for repair and reconstruction of cartilage defects(Chung, Burdick, 2008; Langer, Vacanti, 1993), engineering cartilage with a delicate three dimensional (3D) structure, such as a human ear, remains a great challenge in this field(Ciorba, Martini, 2006; Sterodimas et al., 2009; Zhang, 2010). Since in 1997 Cao *et al*. engineered the cartilage with a shape of human auricle in a nude mouse model(Cao et al., 1997), many researchers have tried to explore further developments of this tissue engineering system, but few of them have succeeded in *in vitro* regeneration of a cartilage construct with a complete and anatomically refined auricle structure(Haisch et al., 2002; Isogai et al., 2004; Kamil et al., 2003; Kamil et al., 2004; Naumann et al., 2003; Neumeister et al., 2006; Shieh et al., 2004; Xu et al., 2005)(Table 1).

One major reason leading to the failure of *in vitro* engineering a cartilage construct with sufficient control over shape is the lack of appropriate scaffolds(Liu et al., 2010). The optimal scaffold used for engineering a cartilage construct with accurate designed shapes should possess at least three characteristics: good biocompatibility for cartilage formation, ease of

being processed into a specific shape, and sufficient mechanical strength for retaining the pre-designed shape during chondrogenesis. Polyglycolic acid (PGA) has proven to be one of the most successful scaffolds for cartilage regeneration(Cui et al., 2009; Frenkel, Di, 2004; Heath, Magari, 1996). Cartilage engineered with the PGA scaffold has structure and composition similar to the native tissue, as demonstrated by histological analysis and cartilage specific matrices(Aufderheide, Athanasiou, 2005; Moran et al., 2003; Yan et al., 2009). However, the most widely used form of PGA material in cartilage engineering is unwoven fiber mesh, which is difficult to be initially prepared into a complicated 3D structure and would most likely fail to maintain its original architecture during subsequent *in vitro* chondrogenesis due to insufficient mechanical support(Gunatillake, Adhikari, 2003; Kim, Mooney, 1998; Moran et al., 2003).

Year	Issue Name	Author	Scaffold	Seeding cells	Shape	Culture
1997	Plastic and Reconstructive Surgery	Cao Yilin et al.	PGA+PLA	Bovine chondrocytes	3-year-old child (partial size)	nude mouse
2002	European Archives of Oto-Rhino-Laryngology	Andreas Haisch et al.	PGA+PLA+Fibrinogen	human nasal septum chondrocytes	Poor shape (silicon stent)	nude mouse (partial)
2003	European Archives of Oto-Rhino-Laryngology	A.Naumann et al.	Hyaff 11	Human nasoseptal chondrocytes	Real size?	Vitro? (partial)
2003	The Laryngoscope	Syed H. Kamil et al.	PGA+PLA	Newborn calf shoulders chondrocytes	Real size Auricle and Nasal Tip	Vitro+ nude rat
2004	Tissue engineering	NORITAKA ISOGAI et al.	PLLA+PCL	Newborn calf shoulders chondrocytes	1-year-old child (partial size)	Nude mouse
2004	Biomaterials	Shyh-Jou Shieh et al.	PGA ,PCL ,P4HB	Adult sheep chondrocytes; rabbit ear cartilage but failed	Poor shape	Vitro+ nude mouse
2004	The Laryngoscope	Kamil,S.H. et al.	Calcium alginate, pluronic, PGA	Chondrocytes	Poor shape(gold stent)	Pig, sheep
2005	Plastic and Reconstructive Surgery	Xu Jianwei et al.	Fibrin	Chondrocytes,perichondrium	Hand sculpted	Nude mouse
2006	Plastic and Reconstructive Surgery	Michael W. Neumeister et al.	Fibrin glue	Chondrocytes femoral vascular pedicle	Poor shape but vascularized (silicone mold)	Rat

Table 1.

To overcome these problems, two crucial issues should be addressed. First, the PGA-based scaffold should be prefabricated into the exact shape of a human ear. Second, the mechanical

strength of the above-mentioned scaffold should be further enhanced so that it can retain the pre-designed shape during *in vitro* chondrogenesis.

Fig. 1. The outline of a human ear

In order to meet these requirements, in the current study, a computer aided design and manufacturing (CAD/CAM) technique was employed to fabricate a set of negative molds, which was then used to press the PGA fibers into the pre-designed ear structure. Furthermore, the mechanical strength of the scaffold was enhanced by coating the PGA fibers with an optimized amount of PLA. Then, the feasibility of engineering a shape controllable ear cartilage *in vitro* was explored by seeding chondrocytes into the optimized scaffolds. In addition, the exactness of the shape of the ear graft was quantitively evaluated by a 3D laser scanning system.

2. Materials and methods

2.1 Preparation of scaffolds with different PLA contents

40 mg of unwoven PGA fibers (provided by Dong Hua University, Shanghai, China) were compressed into a cylinder shape of 13mm in diameter and 1.5mm in thickness. A solution

of 0.3 % PLA (Sigma, St. Louis, MO, USA) in dichloromethane was evenly dropped onto the PGA scaffold, dried in a 65 ^{o}C oven, and weighed. The PLA mass ratio was calculated according to the formula: PLA%= (final mass-original mass)/final mass×100%. The above procedures were repeated until the predetermined PLA mass ratios of 0%, 10%, 20% and 30% were achieved.

2.2 Mechanical analysis of the scaffolds

The mechanical properties of the scaffolds were analyzed by a biomechanical analyzer (Instron-5542, Canton, MA, USA). The scaffold disks were compressed at a constant compressive strain rate of 0.5 mm/min until a maximum of 10% total strain was reached. The maximum compressive force and Young's modulus were determined from the stress-strain curve.

2.3 Biocompatibility evaluation of the scaffolds

Cell seeding: Chondrocytes were isolated from the articular cartilage of newborn swine (2-3weeks old) as described(Rodriguez et al., 1999). The harvested chondrocytes were adjusted to a final concentration of 50×10^{6} cells/mL, and a 200uL cell suspension was pippeted onto each scaffold. The cell-scaffold constructs were then incubated for 5h at 37^{o}C with 95% humidity and 5% CO_2 to allow for complete adhesion of the cells to the scaffolds. Then, the constructs were covered by pre-warmed culture medium and cultured under the same conditions.

Cell adhesion: After 24 hours of incubation, the cell-scaffold constructs were gently transferred into a new 6-well plate for subsequent culture to evaluate cartilage formation. The remaining cells were collected and counted. The cell seeding efficiencies of the scaffolds with different PLA contents were calculated based on the formula: (total cell number-remaining cell number)/ total cell number×100%(Moran et al., 2003).

Scanning electron microscopy (SEM): The constructs were cultured *in vitro* and the attachment and matrix production of the cells on the scaffolds were examined by SEM (Philips XL-30, Amsterdam, Netherlands) after 2 weeks and 8 weeks.

Evaluation of cartilage formation: The constructs were harvested after 8 weeks of culture. The cartilage formation on different scaffolds was evaluated histologically by staining with hematoxylin and eosin (HE) and Safranin O, and immunohistochemically with type II collagen(Zhang, Spector, 2009).

2.4 Mold fabrication by CAD/CAM

A patient's normal ear was scanned by CT to obtain the geometric data. These data were further processed by a CAD system to generate the half-sized mirror image data (both positive and negative) of the normal ear, and the resultant data were input into a CAM system (Spectrum 510, Z Corporation) for the fabrication of the resin models by 3D printing. The negative mold was composed of two parts: the outer part and the inner part. In order to make the mold pressure-loadable, the outer part was replaced by a silicon rubber, which was molded according to the inner part of the resin negative mold.

2.5 Fabrication of ear shaped scaffold

Two hundred milligrams of unwoven PGA fibers were pressed using the negative mold for over 12 hours. A solution of 0.3 % PLA (Sigma, St. Louis, MO, USA) in dichloromethane was

evenly dropped onto the PGA scaffold, dried in a 65 °C oven, weighed, and pressed again with the negative mold. This procedure was repeated until the final PLA mass ratio of 20% was reached. The edge of the scaffold was carefully trimmed according to the shape of the positive mold.

2.6 Three-dimensional laser surface scanning

A 3D laser scanning system was used for the shape analysis(Yu et al., 2009). The surface image data were collected from both the positive mold and the ear shaped scaffolds using a Konica Minolta Vivid 910 and Polygen Editing Tools version 2.21 (Konica Minolta, Tokyo, Japan). These data were further processed by RapidForm 2006 (INUS, Seoul, South Korea) and HP xw6200 (Hewlett Packard, Shanghai, China). The resultant data obtained from the ear-shaped scaffolds were compared to those from the positive mold, which served as a standard. Variations in voxels smaller than 1mm were considered similar, and the number of these similar voxels was divided by the number of total voxels to calculate the similarity level.

2.7 In vitro construction of ear-shaped cartilage

A 1mL aliquot of chondrocyte suspension with a density of 50×10^6 cells/mL was seeded into the ear-shaped scaffold followed by incubating for 5h, according to the cell seeding procedures described above. Then, the construct was gently transferred into a 50mL centrifuge tube for subsequent culture. The culture medium was changed every other day. The constructs were harvested at 4weeks, 8 weeks and 12 weeks for evaluation of shape exactness and cartilage specific histology.

2.8 Statistical analysis

The differences of cell seeding efficiencies (n=6), Young's moduli (n=6), and maximum compressive loadings (n=6) among the four PLA content groups were analyzed using the Student's t-test. A *p*-value less than 0.05 was considered statistically significant.

3. Results

3.1 Mechanical analysis of different scaffolds

The mechanical properties of the scaffolds were analyzed to evaluate the effects of PLA coating with different amount on the mechanical strength. As shown in Figure 2, all the scaffolds had regular cylinder shapes with the same diameter of 13mm (Fig. 2A-2D). No obvious differences in appearance were observed among the PLA/PGA scaffolds with different PLA amounts (Fig. 2B-2D). As expected, the pure PGA group (0% PLA group) showed a flat compressive stress-strain curve close to the X axis, indicating that pure PGA scaffolds had relatively low mechanical strength. With an increase in PLA content, the compressive stress-strain curves became steeper and more linear before the maximum loadings were reached (Fig. 2E), and the compressive moduli (Fig. 2F) as well as maximum loadings (Fig. 2G) also increased. Noticeably, there was a significant increase (over 4 folds) in both compressive moduli and maximum loading in scaffolds fabricated with 20% PLA compared to those with 10% PLA. Furthermore, the scaffold with 20% PLA reached a compressive modulus around 45MPa (45.42±10.52 MPa), which was similar to that of native adult human articular cartilage [19]. As expected, the 30% PLA group achieved the highest maximum loading and Young's modulus in all groups, although no significant difference was observed in Young's modulus between the 20% and 30% groups.

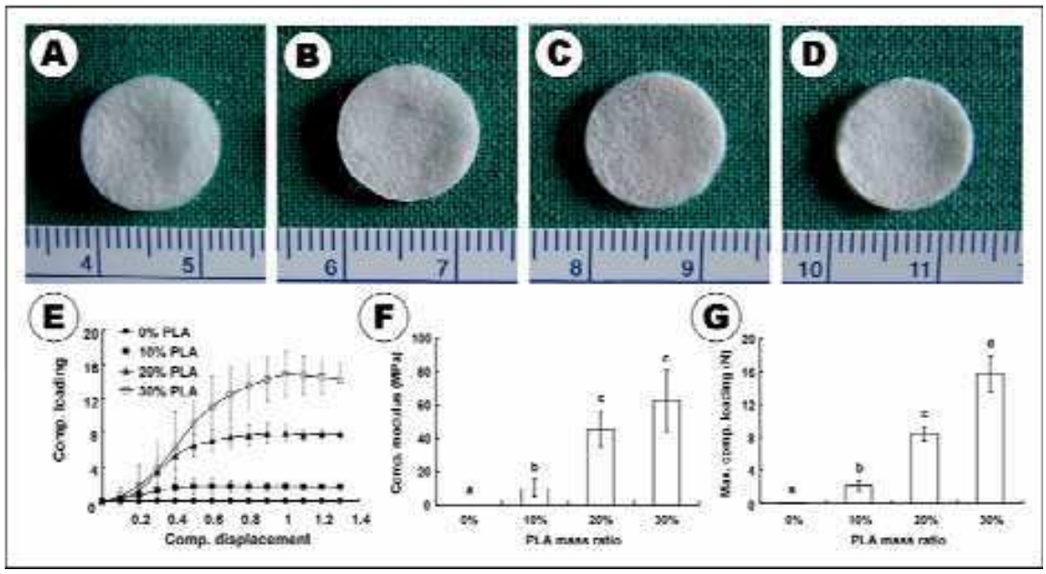

Fig. 2. The influences of PLA contents on mechanical properties. PGA fibers are pressed into a regular cylindrical shape (A). No obvious differences in appearance are observed among the PLA/PGA scaffolds with different PLA ratios of 10% (B), 20% (C), and 30% (D). The scaffolds have different stress-strain curves (E), with significant differences in maximum loading (F) and Young's modulus (G). Different lower-case letters indicate significant differences ($p<0.01$)

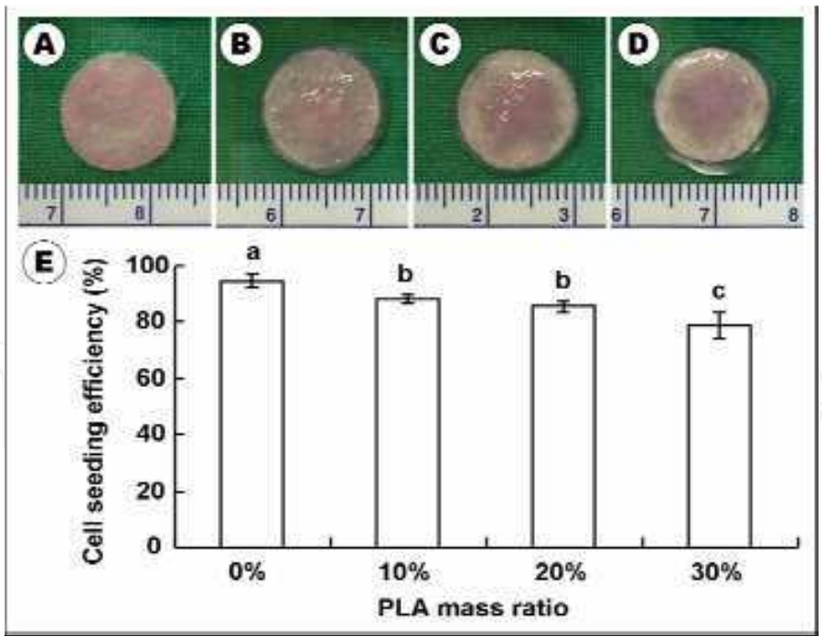

Fig. 3. The influences of PLA contents on cell seeding efficiency. Scaffolds with different PLA contents of 0% (A), 10% (B), 20% (C), and 30% (D) absorb different volumes of the cell suspension. Cell seeding efficiencies decrease with increasing PLA contents in the scaffolds, and a significant decrease is observed in the scaffolds with 30% PLA compared to those with 10% and 20% PLA (E). Different lower-case letters indicate significant differences ($p<0.05$)

3.2 Evaluation of the biocompatibility of the scaffolds with different PLA contents

Cell seeding efficiencies, SEM, and histological examination were performed to evaluate the influence of PLA contents on cell compatibility of the scaffolds and on final cartilage formation. The results showed that the increase in PLA content could lead to the reduction in the ability of the scaffolds to absorb the cell suspensions (Fig. 3A-3D), which may be related to the different pore structures (Fig. 4A-4D) and hydrophobicity of the scaffolds with different PLA contents. Quantitative analysis demonstrated that all the groups with PLA presented significantly lower cell seeding efficiencies compared to the group without PLA ($p<0.05$). Most notably, there was a significant decrease in cell seeding efficiencies in scaffolds with 30% PLA compared to those with 10% and 20% PLA, while no significant differences were observed between the scaffolds with 10% and 20% PLA (Fig. 3E).

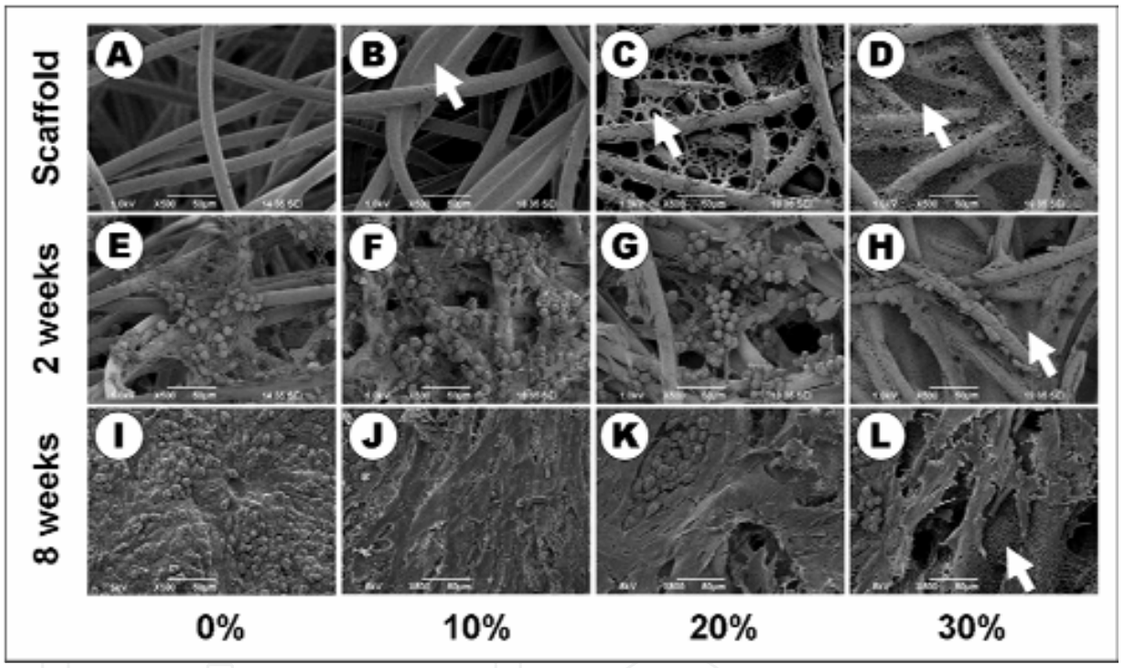

Fig. 4. SEM examination for the influences of PLA contents on cell distribution and ECM production. Scaffolds with different PLA contents show different pore structures (A-D). At 2 weeks, no obvious differences in cell distribution are observed among groups with 0% (E), 10% (F), and 20% (G) PLA, while an obvious decrease in cell number is observed in 30% PLA group (H). At 8 weeks, inferior ECM deposition is observed in 30% PLA group (L) compared to the other groups (I-K). The white arrows indicate the coated PLA

Naturally, the evaluation of final cartilage formation is the most important criterion to determine whether a scaffold can be used for cartilage engineering. As shown in Figure 5, after 8 weeks of *in vitro* culture, homogenous cartilage-like tissue with abundant cartilage-specific extracellular matrices (ECM) was observed in the constructs with 0% (Fig. 5E, 5I, 5M), 10% (Fig. 5F, 5J, 5N), and 20% (Fig. 5G, 5K, 5O) PLA. However, in the group with 30% PLA (Fig. 5H, 5L, 5P), there were high amounts of undegraded scaffold in the constructs, and only sporadic cartilage-like tissues were observed. These findings were consistent with the SEM examinations, which showed an obvious decrease in both cell number and ECM

deposition in 30% PLA group (Fig. 4H, 4L) compared to the other groups (Fig. 4E-4G, 4I-4K). Therefore, these results indicate that 20% but not 30% is an acceptable PLA amount for preparing the scaffolds in terms of cell seeding efficiency, ECM production, and cartilage formation.

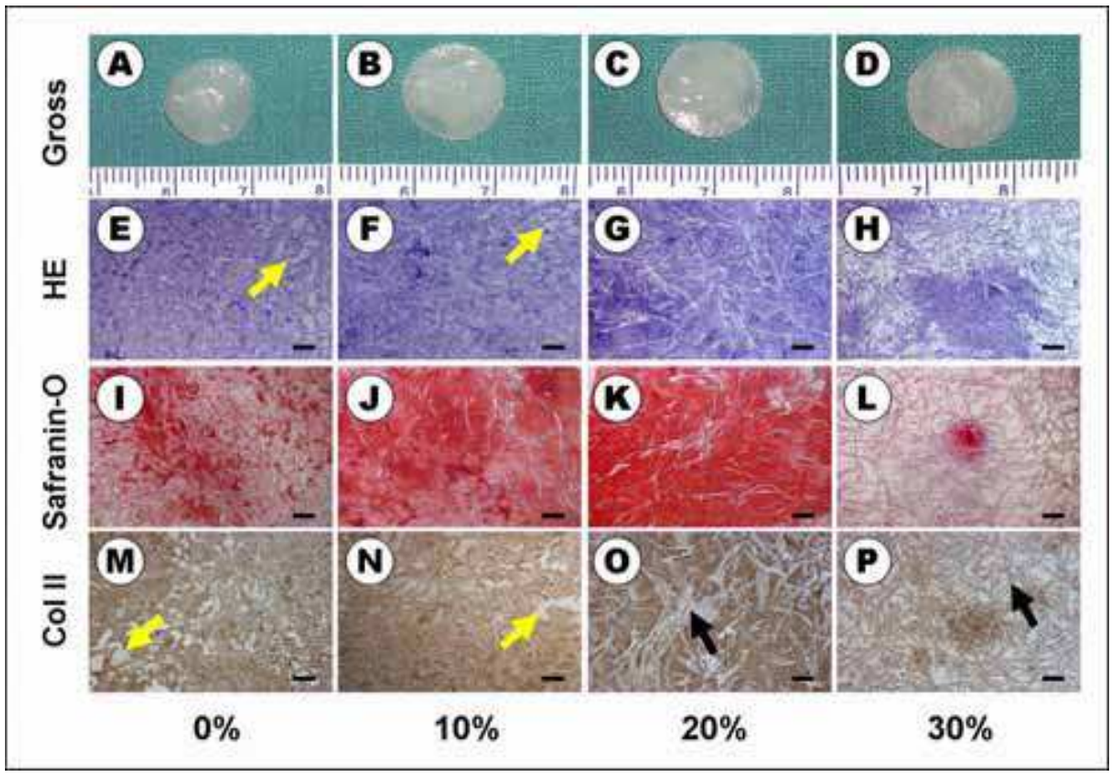

Fig. 5. The influences of PLA contents on cartilage formation. Grossly, the construct without PLA shrinks a little in diameter (A). The constructs that contain PLA basically maintain their original sizes (B-D). Histologically, homogenous cartilage-like tissue is observed in groups with 0% (E, I, M), 10% (F, J, N), and 20% (G, K, O) PLA, except that more compact structures and more undegraded scaffold fibers are observed in 20% PLA group compared with 0% and 10% PLA groups. In the group with 30% PLA (H, L, P), obvious heterogeneous cartilage was observed with an abundance of undegraded scaffolds. The black arrows indicate the undegraded PGA fibers. The yellow arrows indicate void regions caused by fast degradation of the scaffolds. Scale bar = 100μm

3.3 Preparation and shape analysis of ear-shaped scaffold

Because sufficient mechanical strength and good biocompatibility could be achieved in the scaffold with 20% PLA, this formulation was further used for the preparation of the human ear-shaped scaffold. In order to prepare the scaffold into a shape that is mirror-symmetrical to the normal ear, a set of negative molds in half size of an ear (Fig. 6F-6G) was fabricated according to the mirror image (Fig. 6B) of the normal ear (Fig. 6A). The resulting ear-shaped scaffold (Fig. 6H-6J; Fig. 7A, 7E) achieved a similarity level of above 97% compared to the positive mold, the standard for comparison, (Fig. 6C-6E) according to the shape analysis. These results indicate that the mold fabricated by CAD/CAM technology is allowed to accurately fabricate a scaffold into an ear-shape mirror-symmetrical to the normal ear.

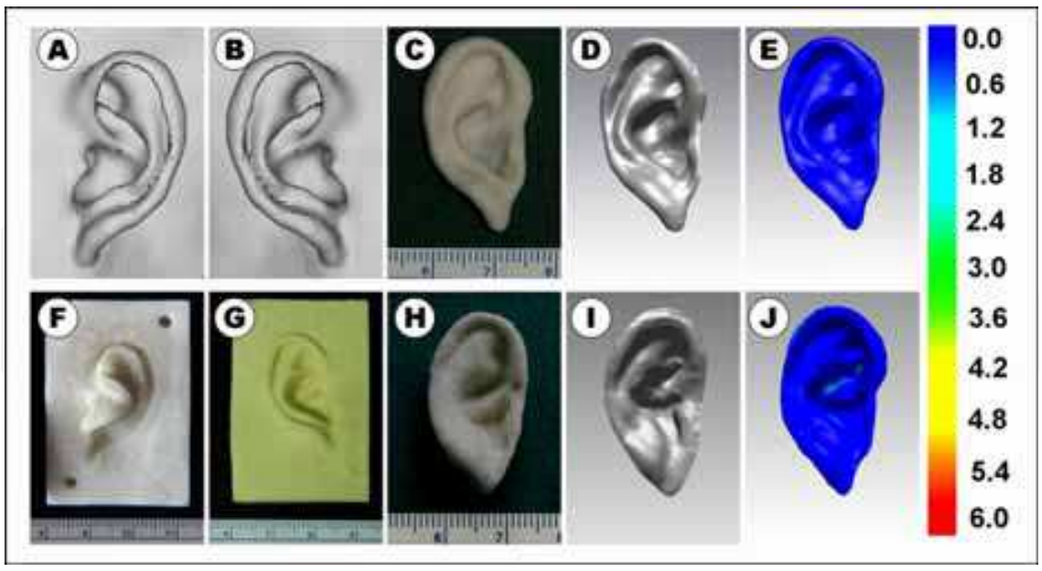

Fig. 6. Preparation and shape analysis of the ear-shaped scaffolds. (A): 3D image of the normal ear; (B): the mirror image of A; (C): The half-sized resin positive mold; (D): laser scan image of C; (E): color map of D; (F): inner part of the resin negative mold fabricated by 3D printing; (G): outer part of the negative mold cast from F with silicon rubber; (H): the ear-shaped PLA/PGA scaffold; (I): laser scan image of H; (J): color map of I compared to D

3.4 Construction of ear-shaped cartilage in vitro

The scaffolds were then used to explore the feasibility of engineering an ear-shaped cartilage *in vitro*. Similarly to the cylindrical scaffold containing 20% PLA, the ear-shaped scaffold also had good compatibility with seeded chondrocytes (data not shown). Most importantly, all the cell-scaffold constructs largely maintained their original ear-like shape during *in vitro* culture, and the shape similarity of the engineered ear grafts was retained at a level of 85.2% at 4 weeks (Fig.7 B, F), 84.0% at 8 weeks (Fig.7 C, G), and 86.2% at 12 weeks (Fig.7 D, H) compared to positive mold, indicating that the mechanical strength of the scaffolds was strong enough to maintain the ear-shape throughout the *in vitro* culture period.

Histologically, the structure of the ear-shaped constructs gradually became compact with prolonged culture time. At 4 weeks, cartilage-like tissue was preliminarily formed despite the presence of many undegraded PGA fibers (Fig.8 A, D, G). At 8 weeks, there was an obvious increase in both cartilage ECM deposition and the number of mature lacuna, although a few PGA fibers remained observable (Fig.8 B, E, H). At 12 weeks, the constructs had completely transformed into cartilage-like tissues with no visible residual PGA (Fig.8 C, F, I), and abundant cartilage ECM and mature lacuna were observed. Furthermore, the ear-shaped neo-cartilage showed fine elasticity with a certain mechanical strength.

4. Discussions

Despite the rapid progress in cartilage engineering, *in vitro* engineering of cartilage with a fine controlled 3D structure, such as a human ear, remains a great challenge due to the lack of appropriate scaffolds. PGA has proven to be one of the most successful scaffolds for cartilage regeneration. However, for *in vitro* engineering of a cartilage with a precise shape, PGA unwoven fibers (the most widely used physical form) still have some drawbacks, such

as the difficulties in controlling an accurate shape and in gaining a proper mechanical strength. In the current study, aided by CAD/CAM technique, the PGA fibers were prepared into the accurate shape of a human ear. Furthermore, by coating with PLA, the scaffold could obtain sufficient mechanical strength to retain the original shape during cell culture until the ear-shaped cartilage was finally formed. These results may provide useful information for future external ear reconstructions by *in vitro* engineered cartilage as well as for the engineering of other tissues with complicated 3D structures.

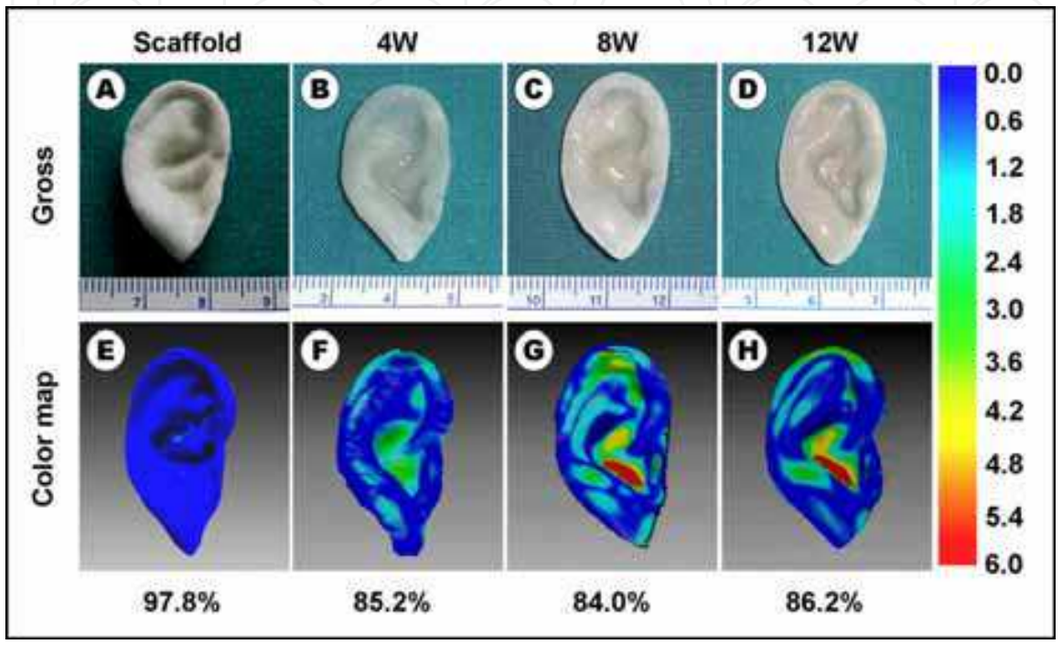

Fig. 7. Shape evaluation of the ear-shaped constructs. The scaffold shows an accurate ear-like structure (A) with a high similarity level compared to the positive mold (E). All the cell-scaffold constructs largely maintain their original ear-like structures at 4weeks (B), 8 weeks (C), and 12 weeks (D). Quantitative analysis show over 84% shape similarity in all the samples (E-H) compared to the positive mold

Preparation of the PGA fibers into an accurate ear structure is the first important step to determine the final shape of the engineered cartilage. To achieve this, a negative mold corresponding to the desired shape is required. Traditionally, the negative mold was fabricated by casting impression materials onto a patient's normal ear(Cao et al., 1997; Isogai et al., 2004), so that the shape of the PGA scaffold prepared by this mold exactly replicated the shape of the ear being casted. However, clinically, the ear aiming to reconstruct should be mirror-symmetrical to the contralateral normal ear. CAD/CAM, as a novel technique, has been widely used for the fabrication of anatomically accurate 3D models(Bill et al., 1995; Ciocca et al., 2007; Erickson et al., 1999; Subburaj et al., 2007). Particularly, this method can accurately perform complicated manipulations of the original 3D data, including Boolean operations, mirror imaging, and scaling(Al et al., 2005; Ciocca, Scotti, 2004; Karayazgan-Saracoglu et al., 2009). CAD/CAM technique was therefore used in the current study for the fabrication of the mirror-image negative mold for a human ear in half size. Using this mold, PGA fibers were able to be accurately prepared into the ear-shaped scaffold that was mirror-symmetrical to the normal ear in half size.

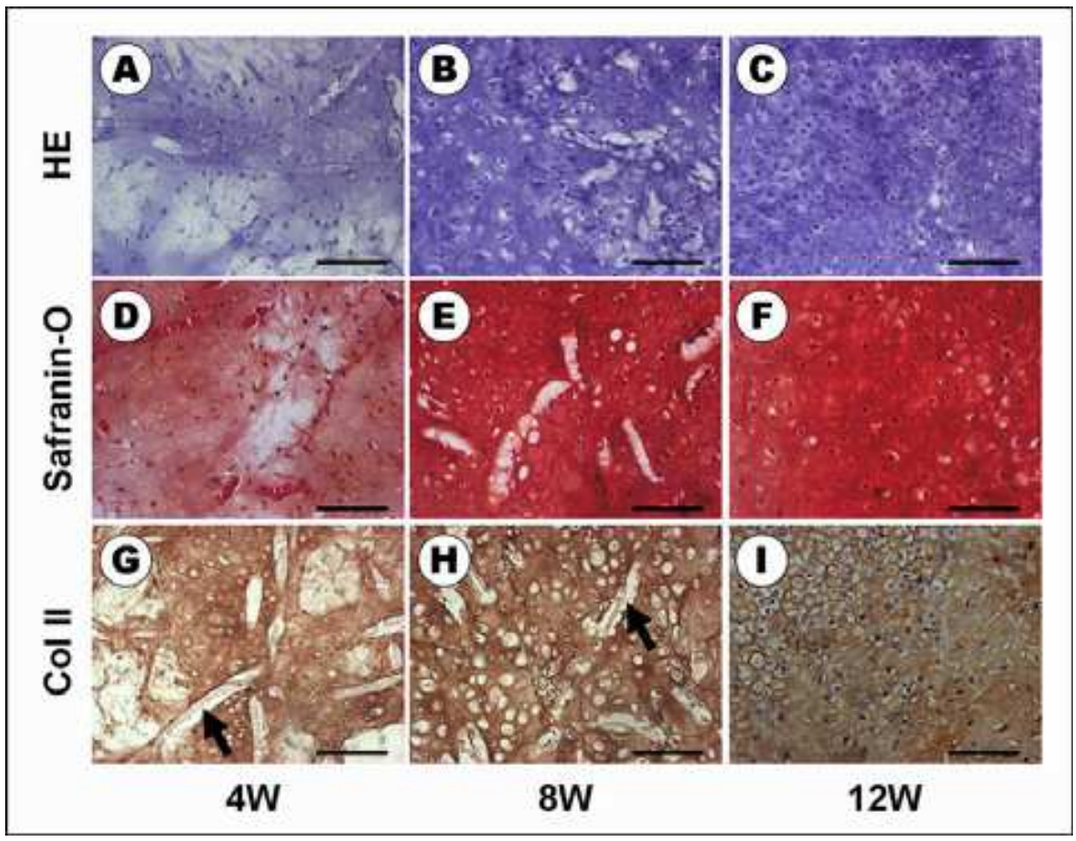

Fig. 8. Histological examinations of the *in vitro* ear-shaped constructs. At 4 weeks, the constructs form heterogeneous cartilage-like tissue along with undegraded PGA fibers (A, D, G). With prolonged culture time, the histological structure of the constructs gradually become compact, accompanied with increased numbers of lacuna structures at 8 weeks (B, E, H). Homogeneous cartilage with abundant ECM and mature lacuna are observed at 12 weeks (C, F, I) with no visible scaffold residuals in the constructs. The black arrows indicate the undegraded PGA fibers. Scale bar = 100μm

After the preparation of the ear-shaped PGA scaffold, the issue of shape retention during *in vitro* chondrogenesis becomes important. The shape maintenance of the cell-scaffold constructs mainly depends on the mechanical strength and degradation rate of the scaffold(Kim et al., 1994). The mechanical strength of PGA scaffold alone is not sufficient for the shape maintenance, and thus PLA coating was used to strengthen its mechanical properties as reported(Cui et al., 2009; Frenkel, Di, 2004; Yang et al., 2001). However, a high amount of PLA in the scaffold would negatively affect cartilage formation because of poor cell compatibility(Moran et al., 2003). Therefore, an appropriate PLA content in the scaffold is important for both cartilage formation and shape maintenance. In the current study, we evaluated the effects of four PLA contents on the scaffolds' mechanical properties and cartilage formation. According to the current results, the mechanical strength of the scaffolds increased with increasing PLA content. However, homogeneous cartilage was only observed in groups with PLA contents of 20% or less. Fortunately, the scaffold with 20% PLA was strong enough to retain the original shape of the cell-scaffold construct until the ear-shaped cartilage was finally formed after 12 weeks.

Besides the mechanical strength, the degradation rate of the scaffold is also an important factor that determines the final shape of engineered tissue. The ideal degradation rate should match the rate of ECM deposition. If the degradation rate of the scaffold is much faster than deposition rate of ECM, the engineered tissue would gradually collapse due to insufficient support, and thus the shape cannot be maintained. According to the histological findings at 8 weeks (Fig.4), the constructs in both 0% and 10% PLA groups had some void regions and lower amounts of residual scaffold, indicating that the degradation rate of the scaffolds in these two groups might be faster than the deposition rate of ECM. In contrast, the constructs in 20% PLA group showed a relatively compact histological structure with more scaffold fibers, indicating the scaffold with 20% PLA has an appropriate degradation rate matching the ECM formation.

In addition, for engineering a complicated structure like a human ear, it is necessary to establish a method to quantitively evaluate the shape exactness of the scaffold as well as to trace the deformation of the constructs during *in vitro* chondrogenesis. 3D laser surface scanning is one of the most popular data acquisition techniques, and has been successfully applied to quantify facial dimensions(Kau, Richmond, 2008; Kau et al., 2005; Toma et al., 2009). It has also been introduced to determine the dimensions of the ear(Coward et al., 2000; Sforza et al., 2005). However, no studies have applied this method to analyze the shape of tissue engineered ear grafts. In the current study, the introduction of 3D laser scanning system provided an effective tool for quantitively evaluating the shape exactness of the ear graft as well as tracing its shape change during *in vitro* engineering.

5. Conclusions

In summary, this study established a method to precisely engineer a cartilage *in vitro* with a shape that is mirror-symmetrical to the normal ear. Additionally, a quantitative system for evaluating the shape exactness of the constructs was established as well. These strategies may provide useful tools for future external ear reconstructions by *in vitro* engineered cartilage as well as for engineering of other tissues with complicated 3D structures. Moreover, the *in vitro* engineering system established in this study may also offer useful references for ear-shaped cartilage construction based on stem cells, since the ectopic chondrogenesis of stem cells requires a long-term induction *in vitro*(Liu et al., 2008). In future studies, we will also investigate the fate of this ear-shaped cartilage after subcutaneous implantation, especially in an immunocompetent animal model.

6. References

Al Mardini M, Ercoli C, Graser GN. 2005. A technique to produce a mirror-image wax pattern of an ear using rapid prototyping technology. *JProsthet Dent*. 94(2):195-8.

Aufderheide AC, Athanasiou KA. 2005. Comparison of scaffolds and culture conditions for tissue engineering of the knee meniscus. *Tissue Eng*. 11(7-8):1095-104.

Beahm EK, Walton RL. 2002. Auricular reconstruction for microtia: part I. Anatomy, embryology, and clinical evaluation. *Plast Reconstr Surg*. 109(7):2473-82; quiz following 2482.

Bill JS, Reuther JF, Dittmann W, et al. 1995. Stereolithography in oral and maxillofacial operation planning. *Int JOral Maxillofac Surg*. 24(1 Pt 2):98-103.

Brent B. 1999. Technical advances in ear reconstruction with autogenous rib cartilage grafts: personal experience with 1200 cases. *Plast Reconstr Surg*. 104(2):319-34; discussion 335-8.

Cao Y, Vacanti JP, Paige KT, et al. 1997. Transplantation of chondrocytes utilizing a polymer-cell construct to produce tissue-engineered cartilage in the shape of a human ear. *Plast Reconstr Surg*. 100(2):297-302; discussion 303-4.

Chung C, Burdick JA. 2008. Engineering cartilage tissue. Adv Drug Deliv Rev. 60(2):243-62.

Ciocca L, Mingucci R, Gassino G, et al. 2007. CAD/CAM ear model and virtual construction of the mold. *JProsthet Dent*. 98(5):339-43.

Ciocca L, Scotti R. 2004. CAD-CAM generated ear cast by means of a laser scanner and rapid prototyping machine. *JProsthet Dent*. 92(6):591-5.

Ciorba A, Martini A. 2006. Tissue engineering and cartilage regeneration for auricular reconstruction. *Int JPediatr Otorhinolaryngol*. 70(9):1507-15.

Coward TJ, Scott BJ, Watson RM, et al. 2000. Laser scanning of the ear identifying the shape and position in subjects with normal facial symmetry. *Int JOral Maxillofac Surg*. 29(1):18-23.

Cui L, Wu Y, Cen L, et al. 2009. Repair of articular cartilage defect in non-weight bearing areas using adipose derived stem cells loaded polyglycolic acid mesh. *Biomaterials*. 30(14):2683-93.

Erickson DM, Chance D, Schmitt S, et al. 1999. An opinion survey of reported benefits from the use of stereolithographic models. *JOral Maxillofac Surg*. 57(9):1040-3.

Frenkel SR, Di Cesare PE. 2004. Scaffolds for articular cartilage repair. *Ann Biomed Eng*. 32(1):26-34.

Gunatillake PA, Adhikari R. 2003. Biodegradable synthetic polymers for tissue engineering. *Eur Cell Mater*. 5:1-16; discussion 16.

Haisch A, Klaring S, Groger A, et al. 2002. A tissue-engineering model for the manufacture of auricular-shaped cartilage implants. *Eur Arch Otorhinolaryngol*. 259(6):316-21.

Heath CA, Magari SR. 1996. Mini-review: Mechanical factors affecting cartilage regeneration in vitro. *Biotechnol Bioeng*. 50(4):430-7.

Isogai N, Asamura S, Higashi T, et al. 2004. Tissue engineering of an auricular cartilage model utilizing cultured chondrocyte-poly(L-lactide-epsilon-caprolactone) scaffolds. *Tissue Eng*. 10(5-6):673-87.

Kamil SH, Kojima K, Vacanti MP, et al. 2003. In vitro tissue engineering to generate a human-sized auricle and nasal tip. *Laryngoscope*. 113(1):90-4.

Kamil SH, Vacanti MP, Aminuddin BS, et al. 2004. Tissue engineering of a human sized and shaped auricle using a mold. *Laryngoscope*. 114(5):867-70.

Karayazgan-Saracoglu B, Gunay Y, Atay A. 2009. Fabrication of an auricular prosthesis using computed tomography and rapid prototyping technique. *JCraniofac Surg*. 20(4):1169-72.

Kau CH, Richmond S. 2008. Three-dimensional analysis of facial morphology surface changes in untreated children from 12 to 14 years of age. *Am JOrthod Dentofacial Orthop*. 134(6):751-60.

Kau CH, Richmond S, Zhurov AI, et al. 2005. Reliability of measuring facial morphology with a 3-dimensional laser scanning system. *Am JOrthod Dentofacial Orthop*. 128(4):424-30.

Kim BS, Mooney DJ. 1998. Engineering smooth muscle tissue with a predefined structure. *J Biomed Mater Res*. 41(2):322-32.

Kim WS, Vacanti JP, Cima L, et al. 1994. Cartilage engineered in predetermined shapes employing cell transplantation on synthetic biodegradable polymers. *Plast Reconstr Surg*. 94(2):233-7; discussion 238-40.

Langer R, Vacanti JP. 1993. Tissue engineering. Science. 260(5110):920-6.
Liu K, Zhou GD, Liu W, et al. 2008. The dependence of in vivo stable ectopic chondrogenesis by human mesenchymal stem cells on chondrogenic differentiation in vitro. *Biomaterials*. 29(14):2183-92.
Liu Y, Zhang L, Zhou G, et al. 2010. In vitro engineering of human ear-shaped cartilage assisted with CAD/CAM technology. *Biomaterials*. 31(8):2176-83.
Moran JM, Pazzano D, Bonassar LJ. 2003. Characterization of polylactic acid-polyglycolic acid composites for cartilage tissue engineering. *Tissue Eng*. 9(1):63-70.
Nagata S. 1993. A new method of total reconstruction of the auricle for microtia. *Plast Reconstr Surg*. 92(2):187-201.
Naumann A, Aigner J, Staudenmaier R, et al. 2003. Clinical aspects and strategy for biomaterial engineering of an auricle based on three-dimensional stereolithography. *Eur Arch Otorhinolaryngol*. 260(10):568-75.
Neumeister MW, Wu T, Chambers C. 2006. Vascularized tissue-engineered ears. *Plast Reconstr Surg*. 117(1):116-22.
Rodriguez A, Cao YL, Ibarra C, et al. 1999. Characteristics of cartilage engineered from human pediatric auricular cartilage. *Plast Reconstr Surg*. 103(4):1111-9.
Sforza C, Dellavia C, Tartaglia GM, et al. 2005. Morphometry of the ear in Down's syndrome subjects. A three-dimensional computerized assessment. *Int J Oral Maxillofac Surg*. 34(5):480-6.
Shieh SJ, Terada S, Vacanti JP. 2004. Tissue engineering auricular reconstruction: in vitro and in vivo studies. *Biomaterials*. 25(9):1545-57.
Sterodimas A, de Faria J, Correa WE, et al. 2009. Tissue engineering and auricular reconstruction: a review. *JPlast Reconstr Aesthet Surg*. 62(4):447-52.
Subburaj K, Nair C, Rajesh S, et al. 2007. Rapid development of auricular prosthesis using CAD and rapid prototyping technologies. *Int J Oral Maxillofac Surg*. 36(10):938-43.
TANZER RC. 1959. Total reconstruction of the external ear. Plast Reconstr Surg. 23(1):1-15.
Toma AM, Zhurov A, Playle R, et al. 2009. Reproducibility of facial soft tissue landmarks on 3D laser-scanned facial images. *Orthod Craniofac Res*. 12(1):33-42.
Walton RL, Beahm EK. 2002. Auricular reconstruction for microtia: Part II. Surgical techniques. *Plast Reconstr Surg*. 110(1):234-49; quiz 250-1, 387.
Xu JW, Johnson TS, Motarjem PM, et al. 2005. Tissue-engineered flexible ear-shaped cartilage. *Plast Reconstr Surg*. 115(6):1633-41.
Yan D, Zhou G, Zhou X, et al. 2009. The impact of low levels of collagen IX and pyridinoline on the mechanical properties of in vitro engineered cartilage. *Biomaterials*. 30(5):814-21.
Yang S, Leong KF, Du Z, et al. 2001. The design of scaffolds for use in tissue engineering. Part I. Traditional factors. *Tissue Eng*. 7(6):679-89.
Yu Z, Mu X, Feng S, et al. 2009. Flip-registration procedure of three-dimensional laser surface scanning images on quantitative evaluation of facial asymmetries. *J Craniofac Surg*. 20(1):157-60.
Zhang L. 2010. It is time to reconstruct human auricle more precisely and microinvasively. *Plast Reconstr Surg*. 125(4):155e-156e.
Zhang L, Spector M. 2009. Comparison of three types of chondrocytes in collagen scaffolds for cartilage tissue engineering. *Biomed Mater*. 4(4):45012.

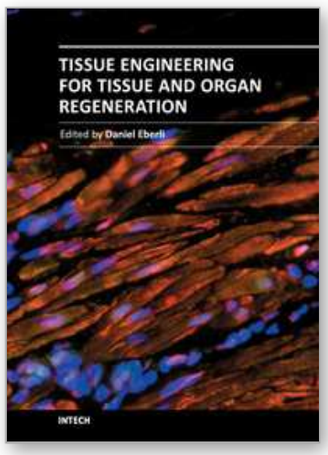

Tissue Engineering for Tissue and Organ Regeneration

Edited by Prof. Daniel Eberli

ISBN 978-953-307-688-1
Hard cover, 454 pages
Publisher InTech
Published online 17, August, 2011
Published in print edition August, 2011

Tissue Engineering may offer new treatment alternatives for organ replacement or repair deteriorated organs. Among the clinical applications of Tissue Engineering are the production of artificial skin for burn patients, tissue engineered trachea, cartilage for knee-replacement procedures, urinary bladder replacement, urethra substitutes and cellular therapies for the treatment of urinary incontinence. The Tissue Engineering approach has major advantages over traditional organ transplantation and circumvents the problem of organ shortage. Tissues reconstructed from readily available biopsy material induce only minimal or no immunogenicity when reimplanted in the patient. This book is aimed at anyone interested in the application of Tissue Engineering in different organ systems. It offers insights into a wide variety of strategies applying the principles of Tissue Engineering to tissue and organ regeneration.

How to reference

In order to correctly reference this scholarly work, feel free to copy and paste the following:

Lu Zhang, Qiong Li, Yu Liu, Guangdong Zhou, Wei Liu and Yilin Cao (2011). Human Ear Cartilage, Tissue Engineering for Tissue and Organ Regeneration, Prof. Daniel Eberli (Ed.), ISBN: 978-953-307-688-1, InTech, Available from: http://www.intechopen.com/books/tissue-engineering-for-tissue-and-organ-regeneration/lu-zhang-qiong-li-yu-liu-guangdong-zhou-wei-liu-and-yilin-cao

INTECH
open science | open minds

InTech Europe
University Campus STeP Ri
Slavka Krautzeka 83/A
51000 Rijeka, Croatia
Phone: +385 (51) 770 447
Fax: +385 (51) 686 166
www.intechopen.com

InTech China
Unit 405, Office Block, Hotel Equatorial Shanghai
No.65, Yan An Road (West), Shanghai, 200040, China
中国上海市延安西路65号上海国际贵都大饭店办公楼405单元
Phone: +86-21-62489820
Fax: +86-21-62489821

© 2011 The Author(s). Licensee IntechOpen. This chapter is distributed under the terms of the Creative Commons Attribution-NonCommercial-ShareAlike-3.0 License, which permits use, distribution and reproduction for non-commercial purposes, provided the original is properly cited and derivative works building on this content are distributed under the same license.

IntechOpen

IntechOpen